Driveline Modeling with Transmission Loss and Robust Torque Observer Design for Dual Clutch Transmission

Taeheon Lee, Dong-Hyun Kim, and Seibum B. Choi, Member, IEEE

***Abstract*—This paper presents a design of driveline torque observer with dual clutch transmission (DCT). A goal of this study is to improve estimation performance of the observer. To increase the observer's performance, it is important to make an accurate driveline model and a robust observer. First, to increase the accuracy of the model, we propose lumped driveline efficiency which is a parameter that expresses driveline transmission loss. In addition, a recursive least square estimation (RLSE) algorithm is proposed to estimate the parameter using driving data. Then, the model is updated using the estimated parameter value. Second, a reduced order observer is proposed to estimate transmitted torques of driveline in both driving and gear shifting process. Moreover, the observer, which is robust against measurement noise and disturbance, is designed through frequency domain analysis. For frequency domain analysis, an eigenstructure assignment method is applied to tune observer gains. Performance of the proposed RLSE algorithm and the observer are verified through simulation and testbench experiments.**

***Index Terms*—Dual clutch transmission, Driveline modeling, Transmission loss, Recursive least square estimation, Torque estimation, Robust torque observer, Eigenstructure assignment.**

I. Introduction

To increase fuel efficiency, a transmission is essential for both internal combustion engine vehicles and parallel hybrid vehicles. Even in electric vehicles, a two-speed transmission is used to increase the torque range and energy efficiency of the motor [1], [2]. There are various types of transmissions, such as automatic transmission (AT), dual clutch transmission (DCT), and continuously variable transmission (CVT). Among them, DCT transmits torques through two clutches which are directly connected to the wheel. Thus, DCT has higher transmission efficiency than AT and higher durability than CVT. Due to these characteristics, DCT is considered to have high potential [3], and many studies have been conducted to examine the characteristics.

The most important part of the gear shift control is to reduce the shock that occurs during gear shifting. Unlike AT, DCT does not have a torque converter to absorb the gear shift shock, so the driver feels the shock directly. The shock is related to the torque transmitted through the driveline during gear shifting. Many studies have been conducted on a model-based gear shift control strategy to reduce the shock. In [4], a gear shift strategy was proposed that controls the engine and clutch cooperatively. Also, [5] proposed a linear quadratic regulator (LQR) method and [6] proposed a control allocation method applied to gear shifting.

There are two things must be done before applying the above model-based control method. The first is increasing the accuracy of the model to describe an actual physical phenomenon well. To describe the actual driveline accurately, it is necessary to have a high order model that describes all parts of the driveline [7], [8]. [7] showed that the driveline can be described as 15 degrees of freedom. However, when the order of the model becomes too high, it becomes complicated to construct a controller. Moreover, accuracy of the model can be improved by additionally modeling the friction generated by each component [9], [10] and transmission loss of the gears [11]–[13]. As above, there are various types of driveline losses, but these are mainly divided into two types [14]–[16]. First is load independent loss. These are kind of spin losses like windage loss, lubrication loss, and etc. It does not change according to the states of the load and has a constant tendency. Second is load dependent loss. These contain meshing loss of gear and bearing loss, and etc. It changes depending on the states of the load such as transmitted torques. If the load dependent losses are not modeled, the error of the model gradually increases as the transmitted torque increases. However, if all the detailed loss models are used for loss modeling, it is difficult to obtain the values of all parameters.

Therefore, it is necessary to make a simplified model, which is called a control-oriented model, for a controller and observer. To make a control-oriented model, [17] proposed a 4th order model and [18] proposed a 3rd order model. In both cases, the model was suitable for configuring a controller and observer due to its low order. However, since transmission losses of the driveline are not considered at all, the model cannot accurately describe the actual driveline. This leads to deterioration of the performance of the model-based controller and observer.

The second thing that must be done before applying the control method is to design the torque observer with robust estimation performance. In production vehicles, there is no torque sensor due to price and packaging issues, so it is not possible to measure the actual torque transmitted through the driveline. Therefore, a design of the torque observer is required for torque-based gear shift control. Many studies have been conducted on designing the torque observer. [19] proposed a nonlinear observer to estimate output shaft torque, and [20] proposed an estimator that used a Kalman filter. However,

T.Lee, D.Kim, and S.B.Choi (Corresponding author) are the Korea Advanced Institute of Science and Technology, 291, Daehak-ro Yuseong-gu, Daejeon, 34141, South Korea (e-mail: pos99126@kaist.ac.kr, kkddh@kaist.ac.kr, sbchoi@kaist.ac.kr).

for designing and verifying the estimator, external resistance torque is assumed to be a known input, which is a limitation of above studies. The difficulties in estimating the torque of an actual vehicle are that the external resistance torque changes according to unknown external road conditions. Another difficult point is that a clutch friction coefficient changes with the temperature [21]–[23] and the slip [24], [25] of the clutch during gear shifting. Therefore, it is difficult to know the actual clutch torque with pre-modeling. Thus, the observer must be able to estimate the output torque and the clutch torque simultaneously. [26] proposed a torque estimator using a full order Luenberger observer, and estimated the torques with an appropriate assumption in each gear shift phase. Also, [27], [28] proposed PI type observer. In [29], an adaptive observer was used to design the torque observer that could adapt to changes in engine torque uncertainty and vehicle inertia. In above cases, stability of the observer was proved. However, since the observer gain was arbitrarily tuned, robust performance was not guaranteed. In this case, disturbance can deteriorate the observer's estimation performance. Therefore, it is important to set the observer gain through frequency domain analysis [30], [31]. Moreover, since a full order Luenberger observer could not decouple the characteristic equation of the measurements and states, it limits the loop shaping of the transfer function. Therefore, it is not able to maximize the performance of the observer.

In this paper, we first propose a new parameter called lumped driveline efficiency to increase the accuracy of control-oriented model. Lumped driveline efficiency represents the ratio between transmitted energy and total energy. Therfore, it is suitable for modeling the load dependent losses. Since the parameter value is an unknown, we propose a recursive least square estimation (RLSE) method to estimate the lumped driveline efficiency using driving data. It also analyzes persistent excitation (PE) condition of the algorithm that guarantees parameter convergence. These proposal are verified through the simulation and testbench experiments.

Second, we propose a reduced order observer to improve estimation performance of the torque. The observer is designed using different models for 1st and 2nd gear driving, torque phase, and inertia phase. Subsequently, frequency domain analysis is performed to ensure robust performance of the observer. Application of the eigenstructure assignment method is proposed for gain tuning of the observer in the frequency domain. Performance of the tuned observer for each phase is verified through the testbench experiments.

The rest of paper is organized as follows. Section 2 proposes the control-oriented model with lumped driveline efficiency and introduces the parameter estimation method using RLSE. Simulation verification is performed for the above method. Section 3 describes the design of the reduced order observer and introduces the gain tuning of the observer using the eigenstructure assignment method. Frequency domain analysis is performed in each gear shift phase. In section 4, performance of the parameter estimation algorithm is verified through testbench experiments. Moreover, we compare the estimated performance between the full order observer and the proposed reduced order observer through the testbench experiments. Conclusions are provided in section 5.

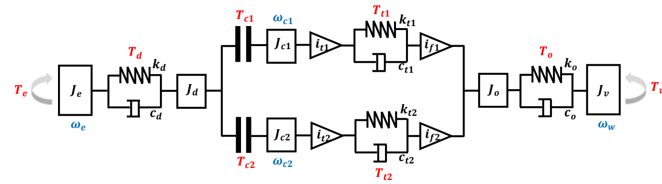

Fig. 1: Conventional driveline model

II. System modeling

A. Conventional driveline model

Fig. 1 shows a conventional driveline model. In Fig. 1, T, ω, J, k, c, i represent torque, angular speed, inertia, torsional stiffness, damping coefficient, and gear ratio. Subscript e, d, c, t, f, o, v are engine, external damper, clutch, transfer shaft, final gear, output shaft, and vehicle. In this paper, only the features of the conventional model are briefly described (See [29] for more details). Fig. 1 depicts transmission process of the torque from the engine to the wheel. A high order model is formed to express all the compliance of the shafts. The model can express all vibrations of each shaft as well as stick-slip phenomenon. However, the controller and observer made from this model have high order and the configuration is complex. In addition, the model has a limitation in that driveline losses such as gear loss and friction are not considered at all.

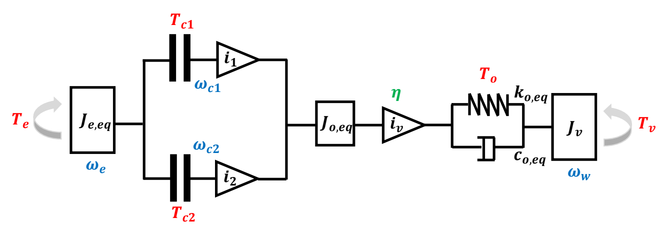

Fig. 2: Control-oriented model with lumped dirveline efficiency

B. Control-oriented model with lumped driveline efficiency

[18] proposed a 3rd order control-oriented model to address the complexity of the conventional model. In [18], the process configuring the control-oriented model was represented. A controller and observer could be simply made from the proposed low order model, but it did not consider driveline losses.

A control-oriented model with lumped driveline efficiency is proposed to solve the above problems. Lumped driveline efficiency refers to the lumped energy transmission losses that can occur in various gears as shown in Fig. 1. The lumped driveline efficiency is expressed as transmission efficiency of the virtual gear located in front of the output shaft as shown in Fig. 2. Gear ratio of the virtual gear (i_v) is assumed to be 1. The control-oriented model with lumped driveline efficiency is configured as in Fig. 2.

In Fig. 2, the torque balance equations of the engine and the clutches are as follows.

$$T_e - T_{c1} - T_{c2} = J_{e,eq}\dot{\omega}_e \tag{1}$$

$$T_{c1} = \left(\begin{array}{cc} T_e - J_{e,eq}\dot{\omega}_e - T_{c2} & (Engaged) \\ \mu_{k1} r_{c1} N_{c1} F_{c1} & (Slipping) \\ 0 & (Disengaged) \end{array} \right. \tag{2}$$

$$T_{c2} = \begin{pmatrix} T_e - J_{e,eq}\dot{\omega}_e - T_{c1} & (Engaged) \\ \mu_{k2} r_{c2} N_{c2} F_{c2} & (Slipping) \\ 0 & (Disengaged) \end{pmatrix} \tag{3}$$

where T_e, T_{c1}, T_{c2} represent the engine torque, clutch 1 torque, and clutch 2 torque. $J_{e,eq}$ is the lumped inertia from the engine to the clutch, and ω_e is the engine speed. μ_k, r, N, F are the dynamic friction coefficient of the clutch, the effective radius, the number of the clutch plate, and the clutch actuator force. In (1), the engine and the torsional damper are expressed as lumped inertia. (2) and (3) represent the transmitted clutch torque according to the state of each clutch.

$$(T_{c1} i_1 + T_{c2} i_2)\,\eta - T_o = J_{o,eq}\eta\frac{\dot{\omega}_{c1}}{i_1} \tag{4}$$

$$\dot{T}_o = c_{o,eq}\left(\frac{\dot{\omega}_{c1}}{i_1} - \dot{\omega}_w\right) + k_{o,eq}\left(\frac{\omega_{c1}}{i_1} - \omega_w\right) \tag{5}$$

$$T_o - T_v = J_v \dot{\omega}_w \tag{6}$$

where T_o, T_v are the output shaft torque and the external resistance torque. ω_{c1}, ω_{c2}, ω_w, i_1 ,i_2, η represent the clutch 1 speed, the clutch 2 speed, the wheel speed, the gear ratio of 1st gear, the gear ratio of 2nd gear, and the lumped driveline efficiency. $J_{o,eq}$, $k_{o,eq}$, $c_{o,eq}$ represent the lumped inertia from the clutch to the output shaft, the equivalent torsional stiffness, and the equivalent torsional damping coefficient. In Fig. 2, since i_v is 1, the energy transmission efficiency of the virtual gear can be expressed as torque transmission efficiency. Based on that, (4) is composed of the torque balance equation considering the lumped driveline efficiency. Since the parameter is multiplied by the torque, it particularly describes lumped load dependent losses, which are varying with the transmitted torque values, in the driveline. It prevents the model error from increasing with the transmitted torques. (5) represents the output shaft compliance model. The methods for obtaining the equivalent torsional stiffness and the damping coefficient were introduced in [18]. (6) indicates the dynamics of the vehicle inertia.

$$T_v = \left(M_v g C_{rr} + M_v g \sin(\theta) + \frac{1}{2}\rho_{air} A_f C_d V^2\right) r_w \tag{7}$$

where M_v, C_{rr}, θ, ρ_{air}, A_f. C_d, V, r_w are the vehicle mass, the rolling resistance coefficient, the road slope, the air density, the vehicle frontal area, the air drag coefficient, the vehicle speed, and the effective radius of the wheel. As in (7), the external resistance torque is expressed as the sum of the rolling resistance, the road grade, and the aerodynamics.

The unknown terms in the above model are the lumped driveline efficiency and the external resistance torque. These values must be estimated from experimental data.

C. RLSE with forgetting factor

RLSE is a famous parameter estimation method. Since RLSE accumulates all past data, it is not suitable for estimating varying parameters. To compensate for that, RLSE with the forgetting factor has been proposed. The forgetting factor can lower the weighting of the past data, so it is used to estimate varying parameters [32]. In [33], [34], RLSE with the forgetting factor was used to estimate road grade and vehicle mass. Since the road grade is a varying term, RLSE with the forgetting factor must be used to estimate both parameters.

In 1st and 2nd gear driving and the gear shifting process, both lumped driveline efficiency and external resistance torque affect the driveline movement. In particular, since both clutches transmit torques during the gear shifting, uncertainty increases and the accuracy of the parameter estimation performance decreases during gear shifting process. Therefore, the parameters are estimated using only driving data in the 1st and 2nd gear where only one clutch is engaged.

Without loss of generality, we assume a 1st gear driving situation. Since clutch 1 is engaged and clutch 2 is disengaged, the speed of the engine and clutch 1 are synchronized and clutch 2 torque is zero. Then, combining (1), (4), and (6), we can obtain the following equation to be used for RLSE.

$$\left(T_e i_1 - \left(J_{e,eq} i_1^2 + J_{o,eq}\right)\frac{\dot{\omega}_e}{i_1}\right)\eta - T_v = J_v\dot{\omega}_w \tag{8}$$

In (8), the engine torque is input, and the engine speed and the wheel speed are measurable states. The lumped driveline efficiency and the external resistance torque are unknown values. In (7), the external resistance torque is composed of the road grade, the rolling resistance, and the aerodynamics.

Assumption 1: Vehicle drives on the road where the road slope does not change rapidly($\dot{\theta} \approx 0$)

In other words, it is assumed that data is obtained for driving on the flat road where the road slope converges to 0 or the gentle hill with a constant road slope. From *Assumption* 1, the road grade term becomes a slowly varying value. In addition, the rolling resistance term varies depending on tire pressure and weight of the vehicle, but it can be regarded as a constant value during driving. Therefore, c_1 expressed as the sum of the above two terms can be assumed as a slowly varying value.

If we combine (7), (8), and $V = r_w\omega_w$, the new equation is as follows.

$$J_v\dot{\omega}_w = \left(T_e i_1 - \left(J_{e,eq} i_1^2 + J_{o,eq}\right)\frac{\dot{\omega}_e}{i_1}\right)\eta - \omega_w^2 c_2 - c_1 \tag{9}$$

where c_1 is the sum of the rolling resistance and the road grade term. c_2 is the lumped aerodynamics coefficient. η, c_1, and c_2 are to be estimated using RLSE with the forgetting factor.

The general formulations of RLSE with the forgetting factor are shown as (10)-(13)

$$y = \theta^T\phi, \quad \varepsilon(k) = y(k) - \hat{y}(k) \tag{10}$$

$$S(k) = \sum_{i=1}^{k}\lambda^{k-i}\left(y(i) - \hat{\theta}^T(k)\,\phi(i)\right)^2 \tag{11}$$

$$F(k) = \frac{1}{\lambda}\left[F(k-1) - \frac{F(k-1)\,\phi(k)\,\phi^T(k)\,F(k-1)}{\lambda + \phi^T(k)\,F(k-1)\,\phi(k)}\right] \tag{12}$$

$$\hat{\theta}(k) = \hat{\theta}(k-1) + F(k-1)\,\phi(k)\,\varepsilon(k) \tag{13}$$

where y, θ, ϕ, ε are the system output, the unknown parameters, the regressors, and the error. S, λ, F represent the cost function, the forgetting factor, and the update gain. λ is from

0 to 1. The larger the λ is, the more past data is accumulated to estimate the parameters. (9) can be expressed in the same form as (10), so RLSE can be applied to (9). In (9), since c_1 changes faster than η and c_2, it is important to set the forgetting factor according to the changing speed of c_1. In addition, there is a derivative term of angular speed in (9). In this case, the signal becomes very noisy due to the derivative value, which has a bad effect on the parameter estimation. Moreover, if unmodeled disturbance acts on the driveline as additional external resistance torques, the parameter estimation performance will be worse. In order to reduce the above bad effects, a moving average filter is applied to y and ϕ values.

Remark 1: In order for $\hat{\theta}$ converging to θ, $\phi(i)(i = 1 \sim k)$ must be linearly independent. If $\phi(i)$ are linearly dependent, these do not satisfy the PE condition in RLSE. So, convergence of $\hat{\theta}$ is not guaranteed. In order to ensure parameter convergence, the condition that $\phi(i)$ are linearly independent in 1st gear driving is as follows.

In 1st gear, a state space model of the driveline is expressed as in (14).

$$
\begin{aligned}
&\dot{x}_1 = A_1 x_1 + B_1 u_1 + E_1 d_1, \quad y_1 = C_1 x_1 \\
&x_1 = \begin{pmatrix} \frac{\omega_e}{i_1} & \omega_w & T_o \end{pmatrix}^T, \; u_1 = T_e, \; d_1 = T_v \\
&A_1 = \begin{bmatrix} 0 & 0 & -\frac{1}{(J_{e,eq} i_1^2 + J_{o,eq})\eta} \\ 0 & 0 & \frac{1}{J_v} \\ k_{o,eq} & -k_{o,eq} & -c_{o,eq}\left(\frac{1}{(J_{e,eq} i_1^2 + J_{o,eq})\eta} + \frac{1}{J_v}\right) \end{bmatrix} \\
&B_1 = \begin{bmatrix} \frac{i_1}{J_{e,eq} i_1^2 + J_{o,eq}} \\ 0 \\ \frac{c_{o,eq} i_1}{J_{e,eq} i_1^2 + J_{o,eq}} \end{bmatrix}, \; C_1 = \begin{bmatrix} 1 & 0 \\ 0 & 1 \\ 0 & 0 \end{bmatrix}^T, \; E_1 = \begin{bmatrix} 0 \\ -\frac{1}{J_v} \\ \frac{c_{o,eq}}{J_v} \end{bmatrix}
\end{aligned} \tag{14}
$$

The transfer function obtained from the state space model in (14) is as follows.

$$
\begin{pmatrix} \frac{\omega_e}{i_1} \\ \omega_w \\ T_o \end{pmatrix} = \begin{bmatrix} G_{11}(s) & G_{12}(s) \\ G_{21}(s) & G_{22}(s) \\ G_{31}(s) & G_{32}(s) \end{bmatrix} \begin{pmatrix} T_e \\ T_v \end{pmatrix} \tag{15}
$$

If (9) and (15) are combined, it is expressed as in (16).

$$
\begin{aligned}
J_v \dot{\omega}_w &= \begin{bmatrix} \eta & c_2 & c_1 \end{bmatrix} \begin{bmatrix} \phi_1 \\ \phi_2 \\ \phi_3 \end{bmatrix} \\
\phi_1 &= \left(i_1 - \left(J_{e,eq} i_1^2 + J_{o,eq}\right) s G_{11}\right) T_e \\
&\quad - \left(J_{e,eq} i_1^2 + J_{o,eq}\right) s G_{12} T_v \\
\phi_2 &= -\left(G_{21} T_e + G_{22} T_v\right)^2, \quad \phi_3 = -1
\end{aligned} \tag{16}
$$

In (16), ϕ_1, ϕ_2, ϕ_3 consist of the transfer functions of T_e and T_v. T_v is uncontrollable and unknown. Therefore, the condition of T_e, which is controllable and known, for the parameter convergence is as follows. In the worst case, if T_e and T_v are constant values, $\phi(i)$ become linearly dependent, so the convergence of $\hat{\theta}$ is not guaranteed. On the other hand, when T_e changes, $\phi(i)$ become linearly independent. Thus, the convergence of $\hat{\theta}$ is guaranteed. Therefore, RLSE is applied using the data obtained when T_e changes. In order to reduce the estimation errors due to sensor noise and disturbance, it is recommended to have a large variation of T_e.

TABLE I: Driveline parameters

Parameter	Value	Parameter	Value
J_e	0.152	k_{t2}	9122
J_d	0.119	c_{t2}	55
J_{c1}	0.01	k_o	17827
J_{c2}	0.012	c_o	87
J_o	0.102	i_{t1}	3.846
J_v	144	i_{f1}	4
k_d	23267	i_{t2}	2
c_d	20	i_{f2}	4.167
k_{t1}	7532	r_w	0.3
c_{t1}	50	M_v	1600

Units are SI derived(kg, m, s)

D. Simulation results

1) Simulation setup and scenario: Simulation describes the testbench using the conventional model Fig. 1, and is constructed with the Simdriveline of Matlab. The inertia, the gear ratio, and the other parameter values are shown in TABLE I. An advantage of the simulation is that it can easily apply aerodynamic torques, which is hard to implement in the testbench experiments. The external resistance torque in the simulation is expressed as in (7). It contains rolling resistance, road load, and aerodynamics. To implement external resistance torque, C_{rr}, ρ_{air}, A_f, C_d are set to 0.02, 1, 2.213, 0.325 in the simulation. Additionally, a 25 rad/s sine wave with magnitude of 10 is applied to the external resistance torque to express unmodeled disturbance. To reflect the actual driveline loss, the loss of each gear is set as load dependent loss [14]–[16]. Therefore, the efficiency of each gear can be represented as weakly varying parameters. The efficiency of each gear is set to a value that increases from 0.95 to 0.97 as the transmitting torque increases. Torques are transmitted through a total of 3 gears at each gear state. Therefore, the overall driveline losses are expressed as the sum of the losses from 3 gears.

In order to guarantee the convergence of the parameters, the

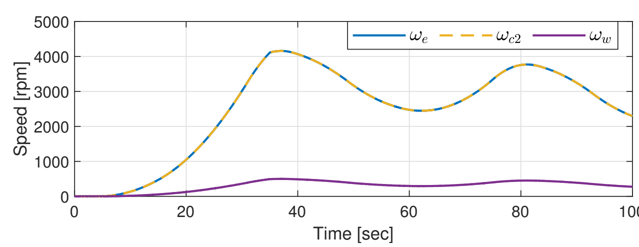

(a)

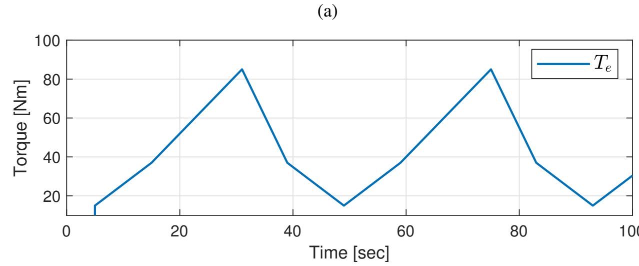

(b)

Fig. 3: Simulation scenario: (a) Speed of each driveline component. (b) Engine torque.

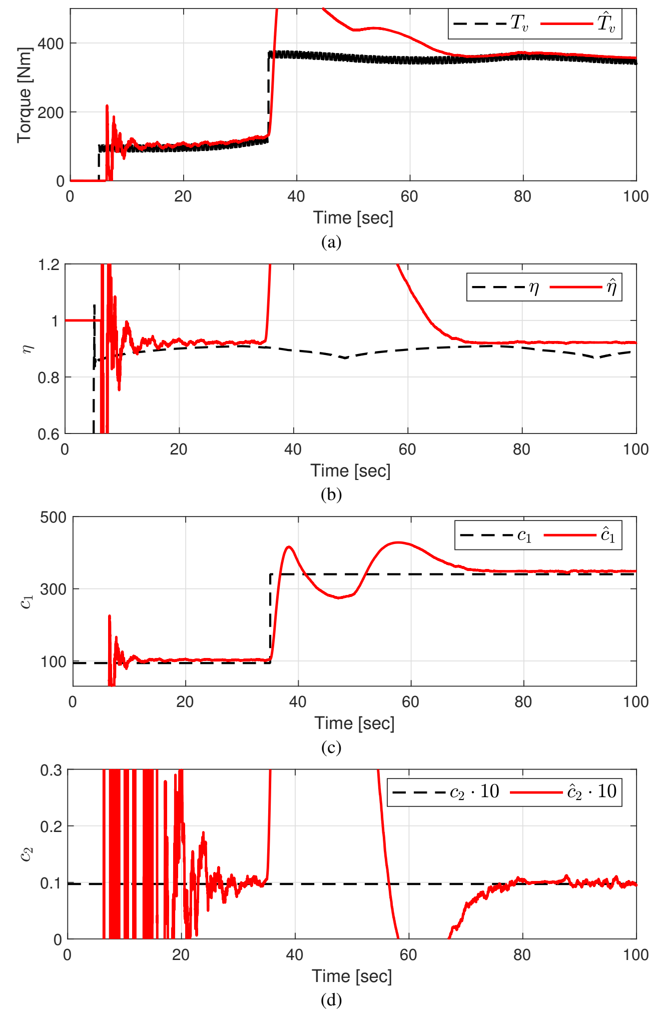

Fig. 4: RLSE results in the simulation: (a) T_v reconstruction. (b) η estimation. (c) c_1 estimation. (d) c_2 estimation.

engine torque is continuously changed after 5 seconds (See $Remark$ 1). In addition, we assume 2nd gear driving which is more affected by the aerodynamic torques in the simulation. To reflect a real driving situation, we set it as a scenario in which the vehicle is driving on a flat road before 35 seconds and then on a gentle hill after 35 seconds. Thus, we set the road slope to 0° before 35 seconds, and changed to 3° after 35 seconds.

2) Results: The speed of the each driveline component and the engine torque are shown in Fig. 3. To estimate the varying parameter, λ must be less than 1. If λ is a large value, more data is used for parameter estimation. Therefore, it has the effect of reducing the varaiance of the estimated parameter due to disturbance and sensor noise. If λ is a small value, less data is used for parameter estimation. Therefore, the variance of the estimated parameter increases from sensor noise and disturbance. However, it has an advantage of fast convergence when the parameter is changed. As above, there is a trade-off relationship to set λ. The way to specify λ is as follows. Gradually decrease λ from a large value (close to 1). After that, according to the changes in λ, it is necessary to check the variance of the converged parameter to know whether estimation performance is acceptable. In this case, λ is set to 0.998. The results of the RLSE are shown in Fig. 4, and the external resistance torque reconstructed with the estimated parameters is also shown in Fig. 4a. In Fig. 4b, η is calculated by multiplying the efficiency of each gear. Since the efficiency of the gear changes every moment, it can be seen that η also changes. $\hat{\eta}$ is convereged to 0.92, which is similar to nominal value. In addition, it takes about 30 seconds for the estimated parameters converging to the changed values. All parameters converge well to its value. Thus, the reconstructed signal also describes the external resistance torque value well.

$Remark$ 2: As the number of estimated parameters increases, various excitation signals must be applied to the system for parameter convergence in RLSE. It means various driving scenarios are needed for parameter estimation. In addition, data can be distorted due to the disturbance and measurement noise in this process. As the number of parameters increases, it becomes more difficult to distinguish the effect of each parameter from distorted data. Thus, it further deteriorates the parameter estimation performance. In order to prevent the deterioration of parameter estimation performance due to the disturbance and measurement noise, it is important to accumulate lots of data by setting the λ close to 1. If λ is set to a high value, the convergence time is increased. However, the lumped driveline efficiency is a parameter that changes slowly and does not need to be estimated in real time. If the estimated value of the lumped driveline efficiency is sufficiently converged, then the control-oriented model is updated using the converged value.

III. Torque observer design

This section presents a design method of the torque observer using the updated model in the previous section. Driveline torques must be estimated in real time through the torque observer.

The clutch involved in transmitting torque changes according to the phase, which is divided into driving situation(1st and 2nd gear driving) and gear shifting(torque phase and inertia phase). Therefore, a state space model of the driveline and the torques to be estimated is changed according to each phase. In this study, observers are constructed using the different model in each phase.

Since gear shifting process is the short time of about 1 second, estimation performance of the observer is very important for precise gear shift control. Thus, it is important to maximize estimation performance of the observer. In many studies, full order Luenberger observers were proposed. In case of the full order observer, it cannot decouple the characteristic

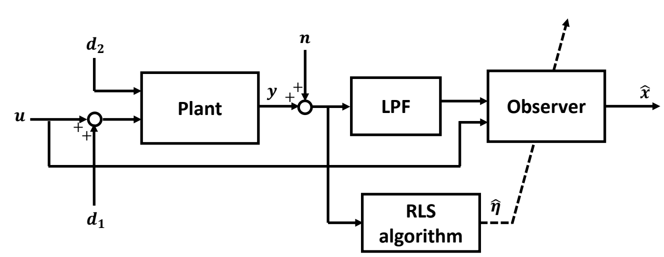

Fig. 5: Overall schematic diagram

equation of measurements and states, so there is a limitation in maximizing the performance of the observer. Therefore, we propose a reduced order observer to compensate for this disadvantage. In order to compensate for the shortcomings of the reduced order observer, which is vulnerable to measurement noise, we practically apply low pass filter (LPF) to the measurement. The overall schematic diagram is shown in Fig. 5.

In order to guarantee robust performance of the observer, we analyze the gain tuning method in the frequency domain and use the eigenstructure assignment method for the gain tuning.

A. Reduced order observer

After arranging the state space model in each phase, a design method of the reduced order observer is proposed.

1) 1st and 2nd gear: In 1st gear, clutch 1 is engaged and clutch 2 is disengaged. Thus, the clutch 2 torque is 0. If the clutch 1 torque is removed in (1)-(6), the equations can be expressed in the state space form as in (14).

In 2nd gear, clutch 1 is disengaged and clutch 2 is engaged. Thus, the clutch 1 torque is 0. In the same way, by removing the clutch 2 torque, the state space form in 2nd gear is constructed as follows.

$$\begin{aligned}
&\dot{x}_2 = A_2 x_2 + B_2 u_2 + E_2 d_2, \quad y_2 = C_2 x_2 \\
&x_2 = \begin{pmatrix} \frac{\omega_e}{i_2} & \omega_w & T_o \end{pmatrix}^T, \; u_2 = T_e, \; d_2 = T_v \\
&A_2 = \begin{bmatrix} 0 & 0 & -\frac{1}{(J_{e,eq} i_2^2 + J_{o,eq})\eta} \\ 0 & 0 & \frac{1}{J_v} \\ k_{o,eq} & -k_{o,eq} & -c_{o,eq}\left(\frac{1}{(J_{e,eq} i_2^2 + J_{o,eq})\eta} + \frac{1}{J_v}\right) \end{bmatrix} \\
&B_2 = \begin{bmatrix} \frac{i_2}{J_{e,eq} i_2^2 + J_{o,eq}} \\ 0 \\ \frac{c_{o,eq} i_2}{J_{e,eq} i_2^2 + J_{o,eq}} \end{bmatrix}, \; C_2 = \begin{bmatrix} 1 & 0 \\ 0 & 1 \\ 0 & 0 \end{bmatrix}^T, \; E_2 = \begin{bmatrix} 0 \\ -\frac{1}{J_v} \\ \frac{c_{o,eq}}{J_v} \end{bmatrix}
\end{aligned} \tag{17}$$

In 1st and 2nd gear, the torques that need to be estimated are T_o and T_v.

2) Torque phase: In the torque phase, clutch 1 is engaged and clutch 2 is slipping. Both clutches are involved in transmitting torque. By removing the clutch 1 torque, it can be arranged in a state space form.

When the clutch is in the slipping state, the friction coefficient changes according to the temperature [21]–[23] and the slip of the clutch [24], [25]. In addition, heat generated from the clutch disc changes characteristics of the cushion spring [21]–[23]. The characteristics of torque transmitted from the clutch changes due to interaction of the several variables. Therefore, it is difficult to describe its characteristics exactly. As a result, the torque actually transmitted from the clutch is different from the nominal model. Therefore, the modeled clutch 2 torque is defined as $T_{c2,n}$ and the torque generated from clutch 2, except the nominal value, is defined as $T_{c2,d}$. For precise gear shift control, the torque additionally transmitted from clutch 2 ($T_{c2,d}$) must be estimated. Thus, torques that need to be estimated in the torque phase are T_o, T_v, $T_{c2,d}$. However, observability is not satisfied in estimating all torques in the torque phase, so we made the following assumption to satisfy the observability condition.

Assumption 2: Since the gear shifting time is as short as 1 second, we assume that the external resistance torque is constant during gear shifting. The estimated external resistance torque in 1st gear is used for the external resistance torque value during gear shifting.

By *Assumption* 2, T_v is regarded as a known input, which is a constant value. Applying this assumption, the state space form is as follows.

$$\begin{aligned}
&\dot{x}_{tp} = A_{tp} x_{tp} + B_{tp} u_{tp} + E_{tp} d_{tp}, \quad y_{tp} = C_{tp} x_{tp} \\
&x_{tp} = \begin{pmatrix} \frac{\omega_e}{i_1} & \omega_w & T_o \end{pmatrix}^T \\
&u_{tp} = \begin{pmatrix} T_e & T_{c2,n} & T_v \end{pmatrix}^T, \; d_{tp} = T_{c2,d} \\
&A_{tp} = \begin{bmatrix} 0 & 0 & -\frac{1}{(J_{e,eq} i_1^2 + J_{o,eq})\eta} \\ 0 & 0 & \frac{1}{J_v} \\ k_{o,eq} & -k_{o,eq} & -c_{o,eq}\left(\frac{1}{(J_{e,eq} i_1^2 + J_{o,eq})\eta} + \frac{1}{J_v}\right) \end{bmatrix} \\
&B_{tp} = \begin{bmatrix} \frac{i_1}{J_{e,eq} i_1^2 + J_{o,eq}} & \frac{-(i_1 - i_2)}{J_{e,eq} i_1^2 + J_{o,eq}} & 0 \\ 0 & 0 & \frac{-1}{J_v} \\ \frac{c_{o,eq} i_1}{J_{e,eq} i_1^2 + J_{o,eq}} & \frac{-c_{o,eq}(i_1 - i_2)}{J_{e,eq} i_1^2 + J_{o,eq}} & \frac{c_{o,eq}}{J_v} \end{bmatrix} \\
&C_{tp} = \begin{bmatrix} 1 & 0 \\ 0 & 1 \\ 0 & 0 \end{bmatrix}^T, \; E_{tp} = \begin{bmatrix} \frac{-(i_1 - i_2)}{J_{e,eq} i_1^2 + J_{o,eq}} \\ 0 \\ \frac{-c_{o,eq}(i_1 - i_2)}{J_{e,eq} i_1^2 + J_{o,eq}} \end{bmatrix}
\end{aligned} \tag{18}$$

In the torque phase, torques that finally need to be estimated are T_o and $T_{c2,d}$.

3) Inertia phase: In the inertia phase, clutch 1 is disengaged and clutch 2 is slipping. Clutch 2 is only involved in transmitting torque. In the same way as in the torque phase, clutch 2 torque is divided into the nominal model value ($T_{c2,n}$) and the undmodeled value ($T_{c2,d}$). Similarly, considering *Assumption* 2, it is expressed as the state space form.

$$\begin{aligned}
&\dot{x}_{ip} = A_{ip} x_{ip} + B_{ip} u_{ip} + E_{ip} d_{ip}, \quad y_{ip} = C_{ip} x_{ip} \\
&x_{ip} = \begin{pmatrix} \omega_e & \frac{\omega_{c2}}{i_2} & \omega_w & T_o \end{pmatrix}^T \\
&u_{ip} = \begin{pmatrix} T_e & T_{c2,n} & T_v \end{pmatrix}^T, \; d_{ip} = T_{c2,d} \\
&A_{ip} = \begin{bmatrix} 0 & 0 & 0 & 0 \\ 0 & 0 & 0 & \frac{-1}{J_{o,eq}\eta} \\ 0 & 0 & 0 & \frac{1}{J_v} \\ 0 & k_{o,eq} & -k_{o,eq} & -c_{o,eq}\left(\frac{1}{J_{o,eq}\eta} + \frac{1}{J_v}\right) \end{bmatrix} \\
&B_{ip} = \begin{bmatrix} \frac{1}{J_{e,eq}} & \frac{-1}{J_{e,eq}} & 0 \\ 0 & \frac{i_2}{J_{o,eq}} & 0 \\ 0 & 0 & \frac{-1}{J_v} \\ 0 & \frac{c_{o,eq} i_2}{J_{o,eq}} & \frac{c_{o,eq}}{J_v} \end{bmatrix} \\
&C_{ip} = \begin{bmatrix} 1 & 0 & 0 \\ 0 & 1 & 0 \\ 0 & 0 & 1 \\ 0 & 0 & 0 \end{bmatrix}^T, \; E_{ip} = \begin{bmatrix} \frac{-1}{J_{e,eq}} \\ \frac{i_2}{J_{o,eq}} \\ 0 \\ \frac{c_{o,eq} i_2}{J_{o,eq}} \end{bmatrix}
\end{aligned} \tag{19}$$

In the inertia phase, the torques that need to be estimated are T_o and $T_{c2,d}$.

States and disturbance are all different in the above 4 cases, but they are arranged in the state space form. If the states and disturbance are augmented to new states, it is organized as follows.

$$\begin{aligned} \begin{pmatrix} \dot{x} \\ \dot{d} \end{pmatrix} &= \begin{bmatrix} A & E \\ 0 & 0 \end{bmatrix} \begin{pmatrix} x \\ d \end{pmatrix} + \begin{bmatrix} B \\ 0 \end{bmatrix} u \\ y &= \begin{bmatrix} C & 0 \end{bmatrix} \begin{pmatrix} x \\ d \end{pmatrix} \end{aligned} \tag{20}$$

To construct the reduced order observer, (20) can be divided into block matrix form as follows.

$$\begin{pmatrix} \dot{x}_a \\ \dot{x}_u \end{pmatrix} = \begin{bmatrix} A_{aa} & A_{au} \\ A_{ua} & A_{uu} \end{bmatrix} \begin{pmatrix} x_a \\ x_u \end{pmatrix} + \begin{bmatrix} B_a \\ B_u \end{bmatrix} u \tag{21}$$

where subscript a and u represent measurable states and unknown states. In each phase, x_a, x_u are arranged as follows. In the 1st gear, x_a, x_u are $(\omega_e/i_1,\ \omega_w)^T$, $(T_o,\ T_v)^T$. In the torque phase, x_a, x_u represent $(\omega_e/i_1,\ \omega_w)^T$, $(T_o,\ T_{c2,d})^T$. In the inertia phase, x_a, x_u express $(\omega_e,\ \omega_{c2}/i_2,\ \omega_w)^T$, $(T_o,\ T_{c2,d})^T$. In the 2nd gear, x_a, x_u are $(\omega_e/i_2,\ \omega_w)^T$, $(T_o,\ T_v)^T$. The formulation of the reduced order observer using (21) is as follows [35].

$$\begin{aligned} \dot{\hat{x}}_u =& A_{ua}x_a + A_{uu}\hat{x}_u + B_u u \\ &+ L\left(\dot{x}_a - A_{aa}x_a - B_a u - A_{au}\hat{x}_u\right) \end{aligned} \tag{22}$$

In (22), the derivative of the measurement is used. In other words, the reduced order observer is sensitive to high frequency noise of the measurement. To solve this problem, a LPF is applied to the measurement as in Fig. 5. The Bode plot analysis for the measurement noise is conducted in the next section. The reduced order observers in each phase are stable when the eigenvalues of the $(A_{uu} - LA_{au})$ matrix are set to be Hurwitz. Moreover, the estimated torques in the previous phase are used as initial conditions of the observer in the next phase.

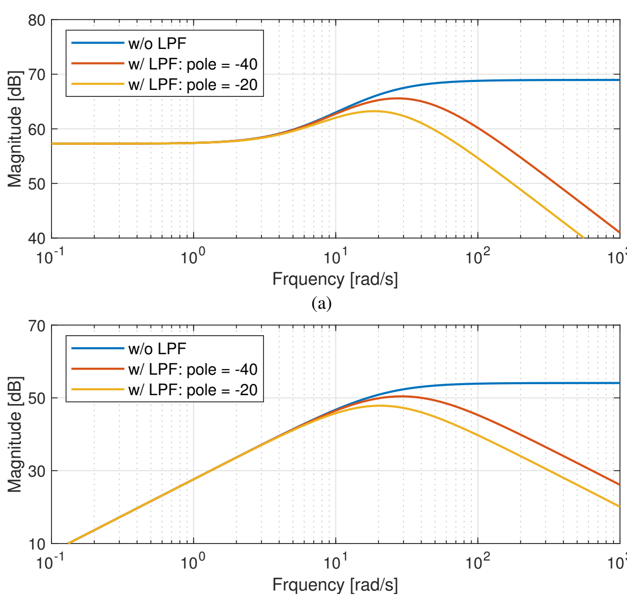

Fig. 6: Bode plot of e/n w/ and w/o LPF in the torque phase: (a) e_1/n_2. (b) e_2/n_2.

B. Observer gain tuning

Fig. 5 is a block diagram showing the relationship between external inputs and estimation errors. d_1 is a matched disturbance, d_2 is a mismatched disturbance, u is a nominal input, and n is sensor noise. First, the transfer functions between the estimation error and each external input must be obtained. Then, according to the target frequency range of the external input, loop shaping should be done in a way that lowers the magnitude of transfer function in the target frequency range.

The characteristics of each transfer function are as follows. Measurement noise contains high frequency range components, so it is important to attenuate the magnitude of the high frequency range. Fig. 6 shows the Bode plot of e_1/n_2 and e_2/n_2 before and after the LPF is applied. The high frequency range can be attenuated by applying the LPF as in Fig. 6. It can be seen that the cutoff frequency of the transfer function changes according to the poles of the LPF. In addition, if the order of the LPF becomes higher, the attenuation slope in the Bode plot increases.

On the other hand, d_1, d_2, and u have low frequency range components. Observer gain tuning should be performed by loop shaping the transfer function of the external input which has a great influence in each phase.

In the case of a linear quadratic (LQ) estimator such as Kalman filter, which is commonly used for gain tuning, it finds an optimal gain according to the Q and R matrix. However, the system poles are randomly changed depending on the Q and R matrix. It has a clear limitation in shaping the loop in the frequency domain by tuning the Q and R matrix.

As another method, a pole placement is widely used for observer gain tuning. In single-input single-output (SISO) system, the observer gain (L) is automatically set when the poles are specified. However, in multi-input multi-output (MIMO) system like driveline, the degree of freedom of L remains even after specifying the system poles. Depending on the remaining degree of freedom of L, the observer performance changes significantly. In order to tune the remaining design freedom, the application of the eigenstructure assignment method [36] that can allocate both eigenvalues and eigenvectors of the observer is proposed for gain tuning. The gain L with the eigenstructure assignment method can be obtained through (23).

$$L = \left(W^{-1}\Lambda W - A_{uu}\right) A_{au}^{-1} \tag{23}$$

where W and Λ are the left eigenmatrix and diagonal matrix of a reduced order observer. In the driveline, A_{au} in each phase are always full rank. Thus, it is possible to do a restriction-free eigenvector assignment where the number of measurements is always equal to or greater than the order of x_u(see [37] for more details). The gain L that can allocate the eigenvalues and eigenvectors arbitrarily is obtained from (23). Therefore, the eigenvalues and eigenvectors can be used as tuning parameters for loop shaping of the reduced order observer.

A brief explanation about the role of the eigenvalues and eigenvectors in the frequency domain is as follows. The eigenvalues indicate the poles of the system. Thus, these are possible to change the cutoff frequency of the transfer function by changing those values. The eigenvectors determine the shape of the Bode plot. The magnitude and combination of the eigenvectors are important factors for the shape of the transfer function. Fig. 7 shows the variation of the transfer functions according to the eigenvectors in the torque phase. It shows the Bode plot of $e/\Delta T_v$ in the torque phase. e_1 and e_2 represent the estimation error of T_o and $T_{c2,d}$. In all 3 cases, the eigenvalues are equal to -10, but the eigenvectors are all different. In case 1, the eigenvectors are $[1\ 0]^T$ and $[0\ 1]^T$. In case 2, the eigenvectors are $[50\ 1]^T$ and $[25\ 1]^T$. In case 3, the eigenvectors are $[1\ 200]^T$ and $[1\ 400]^T$. Despite having the same eigenvalues, it can be seen that various shapes of the transfer functions can be formed according to the eigenvectors. In case 1, there is estimation errors in T_o for ΔT_v of less than 5 rad/s. It means that estimating the constant component of T_v in 1st gear is very important. Moreover, there are almost no errors in $T_{c2,d}$, because it has low magnitude in the Bode plot. In case 2, it can be seen that the magnitude of e_1 is similar to case 1, but the magnitude of e_2 is much larger than case 1. Therefore, estimation error of $T_{c2,d}$ increases. In case 3, the magnitude of e_1 is much larger than case 1 for ΔT_v of 1 to 100 rad/s, but the magnitude of e_2 is similar to case 1. Therefore, estimation error of T_o increases. In summary, proper eigenvector tuning has a great influence on the performance of the observer. It is important to guarantee the observer's robustness through gain tuning in the frequency domain.

The general process of gain tuning is as follows. First, the poles are set to large negative real values for fast response of the observer. Then, loop shaping of the transfer functions is performed by changing the eigenvectors. In this case, both the fast response and robust estimation performance of the observer are satisfied. Second, if the magnitude of the transfer function in the desired frequency range cannot be sufficiently reduced by only tuning the eigenvectors, the observer poles are set to small negative real values. Thus, the response to the undesired external inputs at the corresponding frequency is lowered. Then, eigenvector tuning is performed to reduce the overall magnitude of the Bode plot. In this case, the observer has slow estimation performance. However, the robustness of the observer is improved by lowering the influence on the undesired external inputs that deteriorate the estimation performance.

During the gear shifting process, various torques such as T_e, T_c, and T_v are applied to the driveline. Among them, T_v is torque applied from the outside of the vehicle and cannot be controlled. Therefore, even if an unmodeled disturbance is applied as T_v, the robustness of the observer must be guaranteed. Therefore, among the various external inputs, the Bode plot related with T_v needs to be analyzed.

The following experimental scenarios are designed for verification. In scenario 1, the gear is shifted when a constant T_v is applied. In scenario 2, the gear is shifted while applying an additional 25 rad/s of T_v. Since the additional 25 rad/s of T_v violates $Assumption$ 2, the estimation performance of the observer can be significantly degraded. In addition, when 25 rad/s vibration, which is similar to the resonance frequency of 1st gear driveline, is applied to the system, the estimation performance of the observer may be further degraded. To confirm robust performance of the observer, loop shaping must be performed considering the corresponding vibration components of T_v.

Moreover, the scale of each state may be different in MIMO system. Therefore, normalization between each state must be performed for equivalent analysis. Through normalization, it is possible to know the ratio of the estimation error for each state with respect to disturbance. If loop shaping is conducted with the normalized transfer function, observer gain tuning can be performed considering the ratio of the estimation errors to the state values.

1) 1st and 2nd gear: T_o and T_v are estimated in this phase. Since both states have the same scale, normalization is not

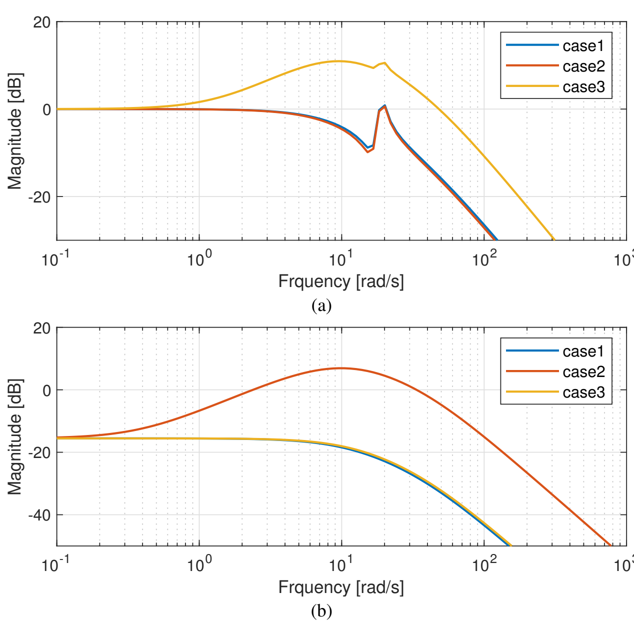

Fig. 7: Bode plot of different eigenvector cases in the torque phase: (a) $e_1/\Delta T_v$. (b) $e_2/\Delta T_v$.

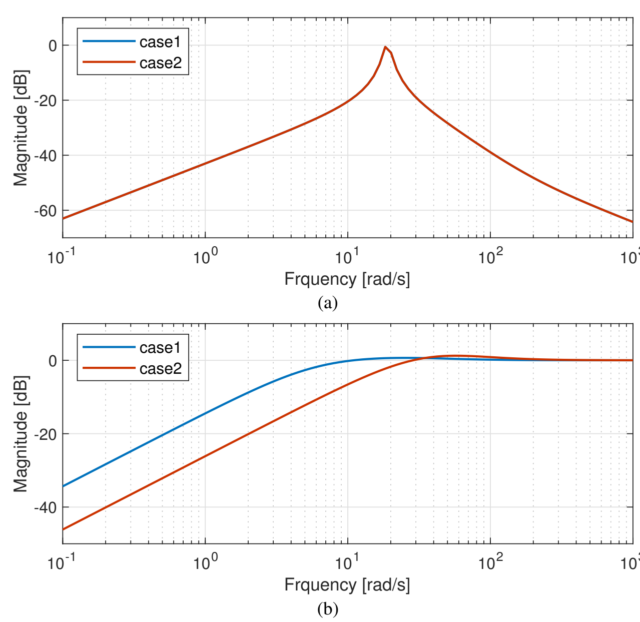

Fig. 8: Bode plot tuning in the 1st and 2nd gear: (a) e_1/T_v. (b) e_2/T_v.

necessary. The Bode plots of e/T_v are shown in Fig. 8. In case 1, the poles are set to -5. In case 2, the poles are set to -40. The eigenvectors of the two cases are $[1\ 0]^T$ and $[0\ 1]^T$. In Fig. 8(a), there is no difference in the two cases. In case 2 of Fig. 8(b), it is possible to estimate the constant component of T_v as well as the 25 rad/s component. On the other hand, it is possible to estimate only the constant component of T_v in case 1 of Fig. 8(b). It can be seen that the estimation performance of case 2 is better. However, due to $Assumption$ 2 in which T_v is kept constant during the gear shifting, it is important to accurately estimate the constant component of T_v during 1st gear. If there are offset estimation errors in constant component of T_v during 1st gear, it causes another estimation error during gear shifting process. Therefore, we set the poles to estimate the constant component of T_v only and use it as an accurate input value during gear shifting. Therefore, case 1 is finally used to reduce the variation of the estimated T_v.

2) Torque phase: T_o and $T_{c2,d}$ are estimated in the torque phase. T_v is regarded as a constant value by $Assumption$ 2. Since the observer in the 1st gear is set to accurately estimate the constant component of T_v, it is enough to ensure the robust performance from the additional vibration component of T_v in the torque phase. Therefore, the Bode plot of the $e/\Delta T_v$ must be analyzed. Since two states have different scale, normailzation is necessary. $T_{c2,d}$ has a scale of $1/i_2$ with respect to the T_o. Therefore, the transfer functions of the $(T_o - \hat{T}_o)/\Delta T_v$ and the normalized $(T_{c2,d} - \hat{T}_{c2,d})/\Delta T_v$ must be analyzed. In addition, the magitudes of the both transfer functions around 25 rad/s is set to be sufficiently lower than 0dB. Fig. 9 shows Bode plot of the $(T_o - \hat{T}_o)/\Delta T_v$ and the normalized $(T_{c2,d} - \hat{T}_{c2,d})/\Delta T_v$. The poles are set to -30 in case 2. With the pole set lower than -25, the magnitude of the Bode plot at around 25 rad/s could not be attenuated by tuning the eigenvectors. Therefore, the poles are set to -5 for lowering the magnitude of the transfer functions, and the eigenvectors are set as $[1\ \ 0]^T$ and $[0\ \ 1]^T$. Case 1 in Fig. 9 shows the finally tuned Bode plot. Moreover, the clutch 2 torque value is estimated using $\hat{T}_{c2} = T_{c2,n} + \hat{T}_{c2,d}$.

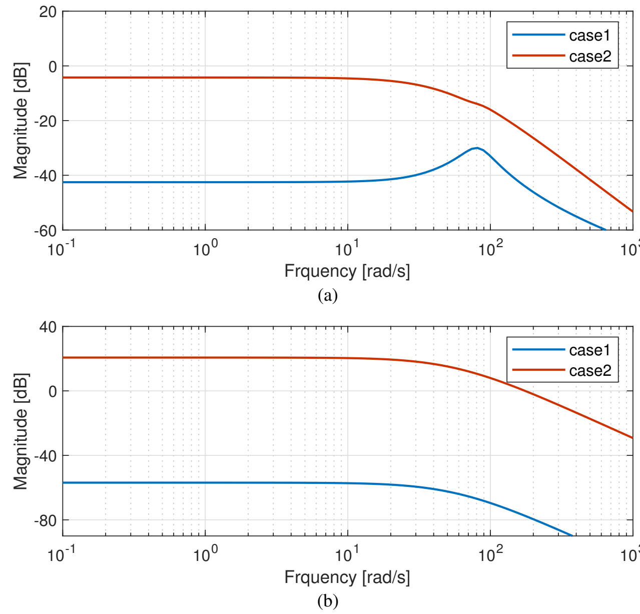

Fig. 10: Bode plot tuning in the inertia phase: (a) $e_1/\Delta T_v$. (b) Normalized $e_2/\Delta T_v$.

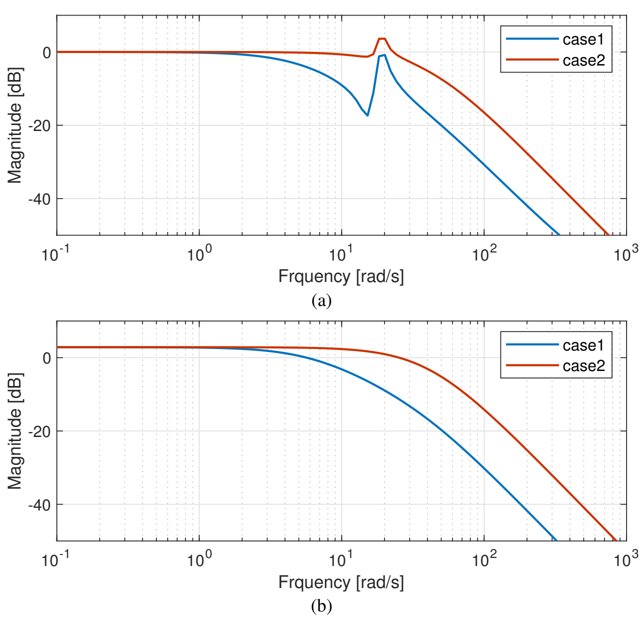

Fig. 9: Bode plot tuning in the torque phase: (a) $e_1/\Delta T_v$. (b) Normalized $e_2/\Delta T_v$.

3) Inertia phase: T_o and $T_{c2,d}$ are estimated in the inertia phase. T_v is regarded as a constant input as in the torque phase. In the same way, the magnitude of the transfer functions of the $(T_o - \hat{T}_o)/\Delta T_v$ and the normalized $(T_{c2,d} - \hat{T}_{c2,d})/\Delta T_v$, around 25 rad/s, needs to be less than 0dB. Fig. 10 shows Bode plot of the $(T_o - \hat{T}_o)/\Delta T_v$ and the normalized $(T_{c2,d} - \hat{T}_{c2,d})/\Delta T_v$. If the poles are set to -80 and the eigenvectors are as $[1\ \ 0]^T$ and $[0\ \ 1]^T$, the transfer function forms a case 1 in Fig. 10. The magnitudes of the estimation errors of T_o and $T_{c2,d}$ become small values. On the other hand, if the poles are set to -80 and eigenvectors are set as $[0.1\ 0.1]^T$ and $[0.2\ 0.1]^T$, it forms a case 2. It can be clear that the magnitudes of both estimation errors become much larger. Therefore, the Bode plot is finally tuned as case 1. It is expected that it has a fast response, and it has a robust performance against 25 rad/s of ΔT_v. As in the torque phase, the clutch 2 torque is estimated using $\hat{T}_{c2} = T_{c2,n} + \hat{T}_{c2,d}$.

IV. Experimental results

A. Experimental setup and scenario

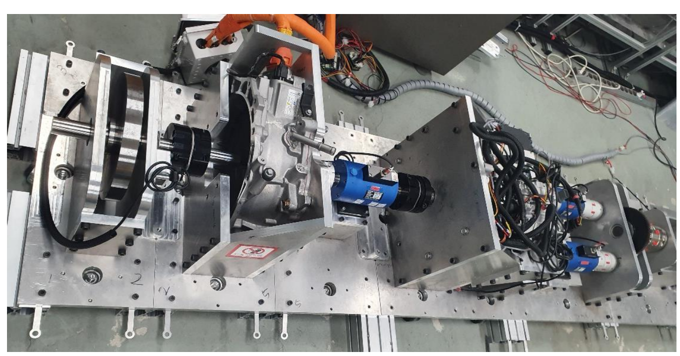

Fig. 11: Testbench configuration

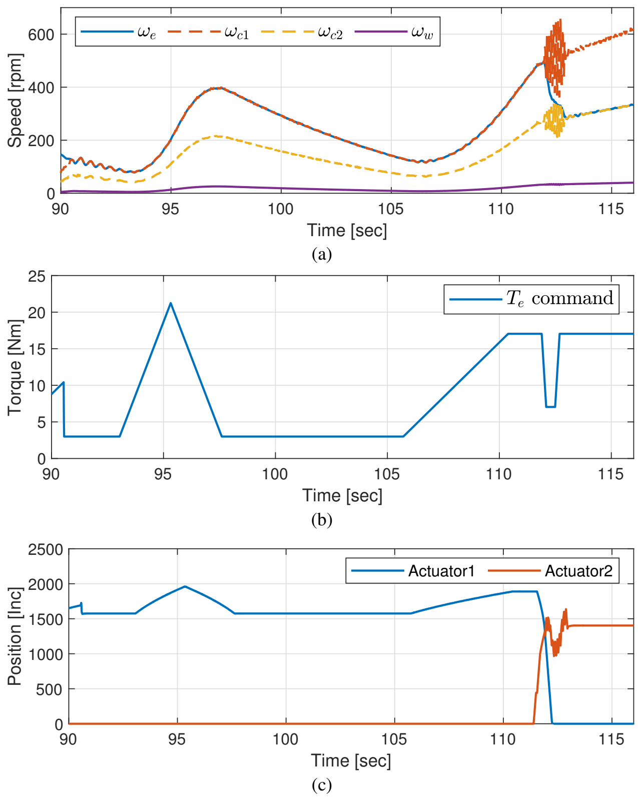

Fig. 12: Testbench experimental scenario 1: (a) Speed of each driveline component. (b) Engine torque command. (c) Actuator position.

The testbench is configured as shown in Fig. 11. Similar to production vehicle, encoders are installed on the engine, clutch 1, clutch 2, and the wheel. Torque sensors are additionally installed on each transfer shaft and behind the engine for verification. Each sensor has a 100Hz sampling rate. Design parameters of the testbench are in TABLE I.

Scenario 1 is as follows. Acceleration and deceleration are performed while the engine torque is changed in 1st gear driving. After that, if the engine speed reaches 450 rpm, the upshfit process from 1st gear to 2nd gear proceeds. In addition, scenario 2 is made to confirm the robustness of the observer. In scenario 2, vibrations of the additional 25 rad/s are applied as T_v. In this situation, the upshift proceeds agiain. Both scenarios are repeated several times.

The results for scenario 1 are shown in Fig. 12, and the results for scenario 2 are shown in Fig. 13. In Fig. 12, the speed graph for 1st and 2nd gear driving has a smooth outline. However, in Fig. 13, the speed graph for 1st and 2nd gear driving has oscillation due to the vibrations of T_v.

B. RLSE results

The RLSE algorithm was applied for scenario 1. Due to the parameter convergence condition, only data were collected when the engine torque changed in 1st gear driving. Unlike in (9), there is no aerodynamic torque in the testbench experiment. Additionaly, there is another viscous torque in the external resistance torque during the testbench experiment. Therefore, (9) can be changed to (24).

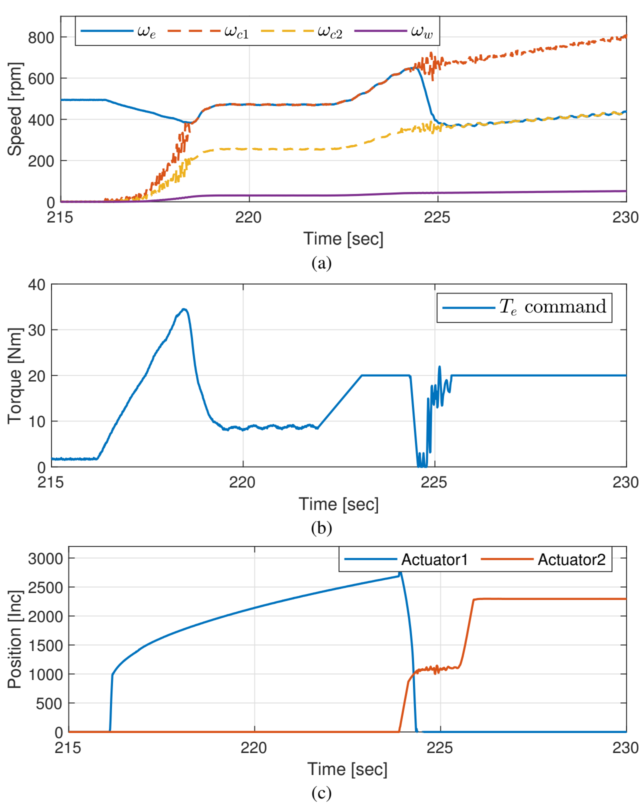

Fig. 13: Testbench experimental scenario 2: (a) Speed of each driveline component. (b) Engine torque command. (c) Actuator position.

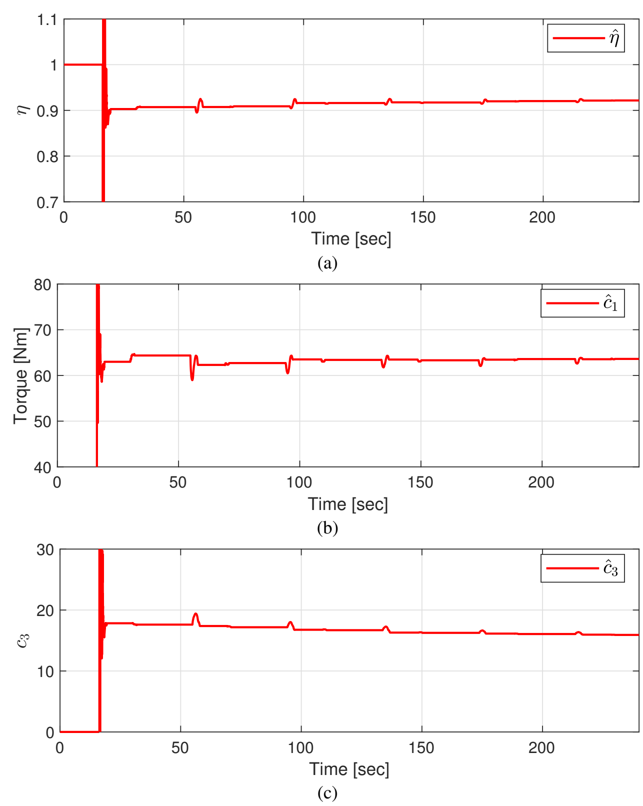

Fig. 14: RLSE results in the experiment: (a) η estimation. (b) c_1 estimation. (c) c_3 estimation.

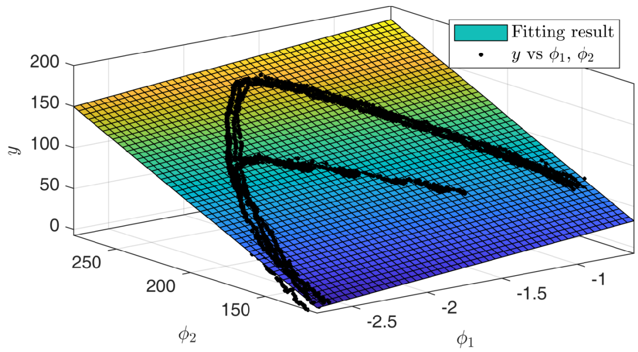

(a)

Fig. 15: LSE results in the experiment

$$J_v\dot{\omega}_w = \left(T_e i_1 - \left(J_{e,eq}i_1^2 + J_{o,eq}\right)\frac{\dot{\omega}_e}{i_1}\right)\eta - \omega_w c_3 - c_1 \quad (24)$$

where c_3 is viscous friction coefficient. η, c_1, c_3 are the parameters to be estimated. Unlike real driving situation, c_1 does not change much during the experiment. If c_1 does not change much, it is not necessary to forget the past data using the forgetting factor. Thus, λ is set to 1 to collect entire experimental data. Fig. 14(a)-14(c) shows the results of the RLSE algorithm using the entire experimental data. The converged values are slightly changed as data accumulates due to sensor noise, model uncertainty, and disturbance. It converges around $\eta = 0.92$, $c_1 = 62$, $c_3 = 16$. Fig. 15 shows least square estimation (LSE) results. R-squared (R^2) between the fitting result and the collected data is 0.984. This confirms that the model reflects the experimental data well. In addition, it can be proven indirectly that the parameter converges well to the actual value. Therefore, accuracy of the updated model, which uses estimated lumped driveline efficiency, can be further improved compared to the conventional control-oriented model which assumes the lumped driveline efficiency as 1.

C. Observer results

Fig. 15 shows the results of the gear shifting in scenario 1. The black lines mean the output torque and the clutch torque data restored from the torque sensor measurements. For comparison, the blue lines mean the torque estimation results of the full order Luenberger observer tuned with the pole placement method. The model used in the full order Luenberger observer is the conventional control-oriented model. The red lines are the results of the proposed reduced order observer. The model used in the reduced order observer is the proposed control-oriented model with estimated lumped driveline efficiency.

Fig. 16(a) shows the torques transmitted from each clutch during gear shifting. Fig. 16(b) shows the output torque. The 1st gear lasts from 111 to 111.5 seconds. From 111.5 to 111.9 seconds is the torque phase. From 111.9 to 112.9 seconds is the inertia phase. From 112.9 to 113.5 seconds is the 2nd gear. In Fig. 16(a), we can see that both observers estimate each clutch torque well during the gear shifting. In Fig. 16(b), the estimated values of both observers have some offsets with the actual output torque during the entire phase. However, since

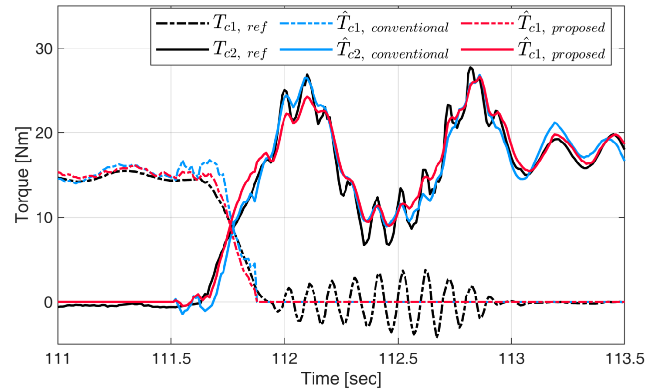

(a)

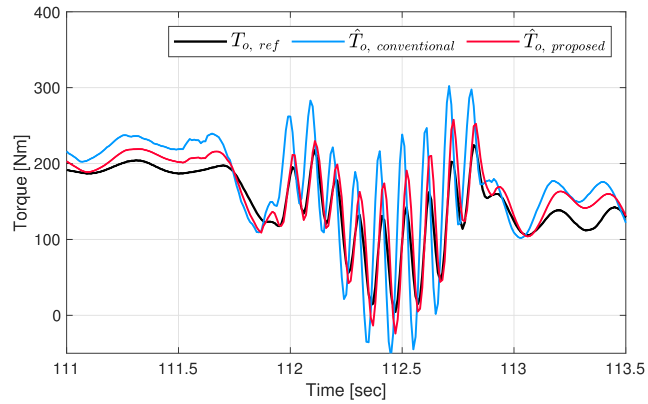

(b)

Fig. 16: Comparison of the observer results in scenario 1: (a) T_{c1} and T_{c2}. (b) T_o

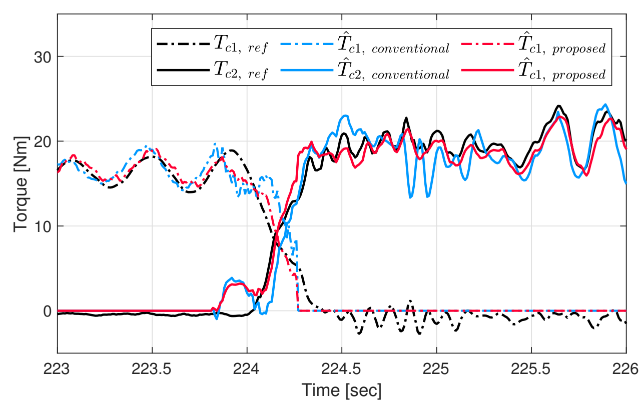

(a)

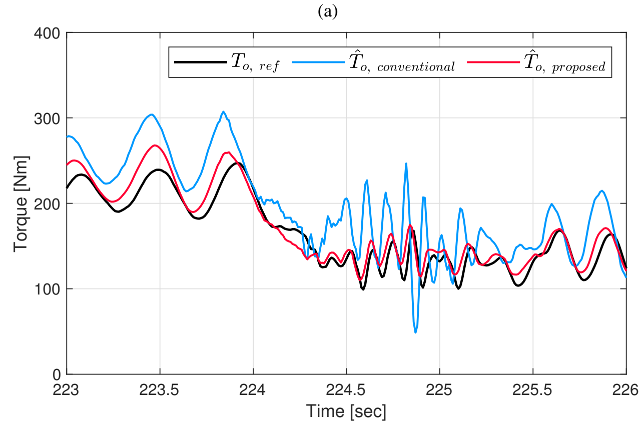

(b)

Fig. 17: Comparison of the observer results in scenario 2: (a) T_{c1} and T_{c2}. (b) T_o.

TABLE II: RMSE of the observer results

RMSE (Nm)		T_{c1}	T_{c2}	T_o
Scenario1	proposed	1.76	1.55	22.27
	conventional	1.96	1.44	61.68
Scenario2	proposed	1.42	1.61	13.17
	conventional	2.09	2.56	44.66

the proposed observer uses the model with estimated lumped driveline efficiency, the output torque estimation performance is slightly improved. The remaining reason for the offset errors is that the model does not contain the friction terms that occur when the each driveline component rotates. This is the limitation of the observer using the proposed control-oriented model.

Fig. 17 shows the results of the gear shifting in scenario 2. Fig. 17(a) shows the torques transmitted from each clutch and Fig. 17(b) shows the output torque. The 1st gear lasts from 223 to 223.8 seconds. From 223.8 to 224.3 seconds is the torque phase. From 224.3 to 225.5 seconds is the inertia phase. From 225.5 to 226 seconds is the 2nd gear. In the torque phase of Fig. 17(a), it can be seen that the proposed observer estimates the clutch 2 torque more accurately compared to the full order observer. If the torque estimation of the clutch 2 is accurate, it is possible to control the off-going clutch (clutch 2) precisely at the end of the torque phase. In addition, in the inertia phase, the proposed observer shows robust performance against the additional external vibrations. Similarly, in Fig. 17(b), the proposed observer estimates the true value better than the full order observer in both phases. A root mean square error (RMSE) of the two observers during the gear shifting are represented in TABLE II. In scenario 1, the RMSE of the clutch torques are similar for the both observers, but the proposed observer has the lower RMSE value in the output torque than the full order observer. In scenario 2, the RMSE of the proposed observer is much smaller than that of the full order observer. Therefore, we can conclude that the proposed observer shows more robust performances against the external input than the conventional full order observer.

V. Conclusion

This paper proposed a new control-oriented model of DCT driveline using lumped driveline efficiency and a new type of driveline torque observer. First, we proposed a new parameter (η) to represent driveline losses occurring in several gears. From the definition of the parameter, it is suitable for representing lumped load dependent losses. It can improve driveline model by decreasing the model error occruing by input torque. In addition, to know the value of the lumped driveline efficiency, we presented a parameter estimation method using RLSE with a forgetting factor. We verified our proposed method through the simulations and experiments.

Second, we designed a reduced order observer to improve the torque estimation performance during gear shifting process. To ensure the torque estimation performance and robustness of the proposed observer, we used gain tuning in the frequency domain through the eigenstructure assignment method. We verified that the proposed observer has better estimation performance and robustness than the conventional observer through the experiments.

In this paper, only design process and the performance verification of the observer for the upshift process were mentioned. Additionally, the above method can also be applied to other gear shift maneuver such as downshift and launch process. The downshift process consists of the 2nd gear, inertia phase, torque phase, and the 1st gear. The launch process consists of idle, inertia phase, and the 1st gear. Therefore, if we construct a model and design the observer according to the order of the each gear shift process, the proposed designing method in this paper can be applied to other gear shift process. The results of this paper are expected to be used to improve the control performance of torque-based gear shift control logic.

Acknowledgment

This research was partly supported by the BK21+ program through the NRF funded by the Ministry of Education of Korea, the Technology Innovation Program (20010263, Development of innovative design for UX environment improvement and commercialization model of wheelchair electric motorization kit with enhanced portability and convenience) funded By the Ministry of Trade, Industry Energy(MOTIE, Korea), the Technology Innovation Program (20014983, Development of autonomous chassis platform for a modular vehicle) funded By the Ministry of Trade, Industry and Energy(MOTIE, Korea), and the National Research Foundation of Korea(NRF) grant funded by the Korea government(MSIP) (No. 2020R1A2B5B01001531).

References

[1] Q. Ren, D. Crolla, and A. Morris, "Effect of transmission design on electric vehicle (ev) performance," in 2009 IEEE vehicle power and propulsion conference. IEEE, 2009, pp. 1260–1265.
[2] B. Gao, Q. Liang, Y. Xiang, L. Guo, and H. Chen, "Gear ratio optimization and shift control of 2-speed i-amt in electric vehicle," Mechanical Systems and Signal Processing, vol. 50, pp. 615–631, 2015.
[3] B. Matthes, "Dual clutch transmissions–lessons learned and future potential," SAE transactions, pp. 941–952, 2005.
[4] M. Pettersson and L. Nielsen, "Gear shifting by engine control," IEEE Transactions on Control Systems Technology, vol. 8, no. 3, pp. 495–507, 2000.
[5] A. Haj-Fraj and F. Pfeiffer, "Optimal control of gear shift operations in automatic transmissions," Journal of the Franklin Institute, vol. 338, no. 2-3, pp. 371–390, 2001.
[6] S. Kim, J. Oh, and S. Choi, "Gear shift control of a dual-clutch transmission using optimal control allocation," Mechanism and Machine Theory, vol. 113, pp. 109–125, 2017.
[7] P. D. Walker and N. Zhang, "Modelling of dual clutch transmission equipped powertrains for shift transient simulations," Mechanism and Machine Theory, vol. 60, pp. 47–59, 2013.
[8] P. Walker, B. Zhu, and N. Zhang, "Powertrain dynamics and control of a two speed dual clutch transmission for electric vehicles," Mechanical Systems and Signal Processing, vol. 85, pp. 1–15, 2017.
[9] X. Zhou, P. Walker, N. Zhang, B. Zhu, and J. Ruan, "Numerical and experimental investigation of drag torque in a two-speed dual clutch transmission," Mechanism and Machine Theory, vol. 79, pp. 46–63, 2014.
[10] Z. Zhao, L. He, Z. Zheng, Y. Yang, and C. Wu, "Self-adaptive optimal control of dry dual clutch transmission (dct) during starting process," Mechanical Systems and Signal Processing, vol. 68, pp. 504–522, 2016.
[11] D. Kim, H. Peng, S. Bai, and J. M. Maguire, "Control of integrated powertrain with electronic throttle and automatic transmission," IEEE Transactions on Control Systems Technology, vol. 15, no. 3, pp. 474–482, 2007.

[12] W. Zhang and X. Guo, "Analysis and modeling of transmission efficiency of vehicle driveline," SAE Technical Paper, Tech. Rep., 2014.
[13] D. Kim, H. Peng, S. Bai, and J. M. Maguire, "Control of integrated powertrain with electronic throttle and automatic transmission," IEEE Transactions on Control Systems Technology, vol. 15, no. 3, pp. 474–482, 2007.
[14] C. Pelchen, C. Schweiger, and M. Otter, "Modeling and simulating the efficiency of gearboxes and of planetary gearboxes," in Proceedings of 2nd International Modelica Conference, 2002, pp. 257–266.
[15] C. Yenti, S. Phongsupasamit, and C. Ratanasumawong, "Analytical and experimental investigation of parameters affecting sliding loss in a spur gear pair," Engineering Journal, vol. 17, no. 1, pp. 79–94, 2013.
[16] C. Wang, S.-r. Wang, and G.-q. Wang, "A method for calculating gear meshing efficiency by measured data from gear test machine," Measurement, vol. 119, pp. 97–101, 2018.
[17] M. Kulkarni, T. Shim, and Y. Zhang, "Shift dynamics and control of dual-clutch transmissions," Mechanism and machine theory, vol. 42, no. 2, pp. 168–182, 2007.
[18] S. Kim and S. Choi, "Control-oriented modeling and torque estimations for vehicle driveline with dual-clutch transmission," Mechanism and Machine Theory, vol. 121, pp. 633–649, 2018.
[19] R. Masmoudi and J. Hedrick, "Estimation of vehicle shaft torque using nonlinear observers," 1992.
[20] H. Hao, T. Lu, and J. Zhang, "Estimation of transmitted torques in dual-clutch transmission systems," Insight-Non-Destructive Testing and Condition Monitoring, vol. 57, no. 8, pp. 464–471, 2015.
[21] M. Hoic, Z. Herold, N. Kranjcevic, J. Deur, and V. Ivanovic, "Experimental characterization and modeling of dry dual clutch thermal expansion effects," SAE International Journal of Passenger Cars-Mechanical Systems, vol. 6, no. 2013-01-0818, pp. 775–785, 2013.
[22] N. Cappetti, M. Pisaturo, and A. Senatore, "Modelling the cushion spring characteristic to enhance the automated dry-clutch performance: The temperature effect," Proceedings of the Institution of Mechanical Engineers, Part D: Journal of Automobile Engineering, vol. 226, no. 11, pp. 1472–1482, 2012.
[23] A. Myklebust and L. Eriksson, "Modeling, observability, and estimation of thermal effects and aging on transmitted torque in a heavy duty truck with a dry clutch," IEEE/ASME transactions on mechatronics, vol. 20, no. 1, pp. 61–72, 2014.
[24] A. Senatore, V. D'Agostino, R. Di Giuda, and V. Petrone, "Experimental investigation and neural network prediction of brakes and clutch material frictional behaviour considering the sliding acceleration influence," Tribology International, vol. 44, no. 10, pp. 1199–1207, 2011.
[25] F. Vasca, L. Iannelli, A. Senatore, and G. Reale, "Torque transmissibility assessment for automotive dry-clutch engagement," IEEE/ASME transactions on Mechatronics, vol. 16, no. 3, pp. 564–573, 2010.
[26] S. Kim, J. J. Oh, and S. B. Choi, "Driveline torque estimations for a ground vehicle with dual-clutch transmission," IEEE Transactions on Vehicular Technology, vol. 67, no. 3, pp. 1977–1989, 2017.
[27] J. J. Oh and S. B. Choi, "Real-time estimation of transmitted torque on each clutch for ground vehicles with dual clutch transmission," IEEE/ASME Transactions on Mechatronics, vol. 20, no. 1, pp. 24–36, 2014.
[28] J. Park, S. Choi, J. Oh, and J. Eo, "Adaptive torque tracking control during slip engagement of a dry clutch in vehicle powertrain," Mechanism and Machine Theory, vol. 134, pp. 249–266, 2019.
[29] J. J. Oh, S. B. Choi, and J. Kim, "Driveline modeling and estimation of individual clutch torque during gear shifts for dual clutch transmission," Mechatronics, vol. 24, no. 5, pp. 449–463, 2014.
[30] K.-S. Kim, K.-H. Rew, and S. Kim, "Disturbance observer for estimating higher order disturbances in time series expansion," IEEE Transactions on automatic control, vol. 55, no. 8, pp. 1905–1911, 2010.
[31] H. J. Marquez, "A frequency domain approach to state estimation," Journal of the Franklin Institute, vol. 340, no. 2, pp. 147–157, 2003.
[32] J. Jiang and Y. Zhang, "A revisit to block and recursive least squares for parameter estimation," Computers & Electrical Engineering, vol. 30, no. 5, pp. 403–416, 2004.
[33] A. Vahidi, A. Stefanopoulou, and H. Peng, "Recursive least squares with forgetting for online estimation of vehicle mass and road grade: theory and experiments," Vehicle System Dynamics, vol. 43, no. 1, pp. 31–55, 2005.
[34] Z. Zhao, X. Li, L. He, C. Wu, and J. K. Hedrick, "Estimation of torques transmitted by twin-clutch of dry dual-clutch transmission during vehicle's launching process," IEEE transactions on vehicular technology, vol. 66, no. 6, pp. 4727–4741, 2016.
[35] D. Luenberger, "An introduction to observers," IEEE Transactions on automatic control, vol. 16, no. 6, pp. 596–602, 1971.
[36] A. Andry, E. Shapiro, and J. Chung, "Eigenstructure assignment for linear systems," IEEE transactions on aerospace and electronic systems, no. 5, pp. 711–729, 1983.
[37] M. Fahmy and I. Khalifa, "Parametric eigenvalue-eigenvector assignment in reduced-order observer design," International journal of systems science, vol. 20, no. 6, pp. 987–1001, 1989.

Taeheon Lee received his B.S. and M.S. degrees in mechanical engineering from Korea Advanced Institute of Science and Technology (KAIST), Daejeon, Korea, where he is currently working toward his Ph.D. degree. His research interests include powertrain modeling and control, hybrid vehicle powertrain, vehicle dynamics and control, and control theory.

Dong-Hyun Kim received the B.S. degree in mechanical engineering from Pusan National University, Busan, Korea, in 2016, the M.S. degree in mechanical engineering from the Korea Advanced Institute of Science and Technology (KAIST), Daejeon, Korea in 2018, and the Ph.D. degree in mechanical engineering from KAIST, in 2022. His research interests energy efficient powertrain, design and control of dual-clutch transmission, uncertainty estimation with nonlinear disturbance observer and powertrain development based on electric vehicle.

Seibum.B.Choi received B.S. degree in mechanical engineering from Seoul National University, Korea, M.S. degree in mechanical engineering from Korea Advanced Institute of Science and Technology (KAIST), Korea, and the Ph.D. degree in controls from the University of California, Berkeley in 1993. Since 2006, he has been with the faculty of the Mechanical Engineering department at KAIST. His research interests include fuel saving technology, vehicle dynamics and control, and application of self-energizing mechanism.